NORTHWEST AFRICA (NWA) 13467: A NEW AUGITE-RICH SHERGOTTITE? L. G. Staddon[1*], J. R. Darling[1], J. Dunlop[1], and N. R. Stephen[2]. [1]School of the Environment, Geography and Geoscience, University of Portsmouth, UK; *leanne.staddon@port.ac.uk. [2]Plymouth Electron Microscopy Centre, Plymouth University, UK.

Introduction: The last decade has seen a significant increase in the number and petrological diversity of martian meteorites [1]. This increased lithological diversity includes regolith breccia Northwest Africa (NWA) 7034 and pairings [2], augite-rich shergottites NWA 8159 [3] and NWA 7635 [4], gabbroic shergottites [5], and a unique pigeonite-rich shergottite [6]. Petrological variability is often also linked to greater chronological diversity; augite-rich shergottites formed at ~2400 Ma [3,4], while NWA 7034 yields zircon and baddeleyite grains with previously unsampled age populations and source reservoirs [7]. Thus, investigation of petrologically distinct martian meteorites may yield important insights into martian crustal and mantle processes. Here, we present preliminary data for NWA 13467, an 80 gram fusion-crusted stone purchased in Morocco in 2020 (Fig. 1). While originally characterized as a micro-gabbroic shergottite [8], we highlight physical and chemical compositions that reveal affinities of NWA 13467 to previously described augite-rich shergottites.

Fig. 1: *50 gram portion cut from the fusion-crusted main mass of Northwest Africa (NWA) 13467. Images courtesy of Sean Mahoney.*

Methods: Two slices of NWA 13467 totaling ~5 grams were acquired for this study, with ~1.5 grams mounted in epoxy for petrological investigation. Electron imaging and phase identification were undertaken using a Zeiss EVO MA10 LaB_6 SEM at the University of Portsmouth. Electron probe microanalysis (EPMA) measurements were conducted using a CAMECA SX100 electron probe at the University of Bristol. Analyses were undertaken at 20 kV with a probe current of 20nA for silicates and oxides, and 10 nA with a ~6 µm beam diameter for glassy phases.

Results: NWA 13467 is fine-grained (≤600 µm), with an equigranular to variably intergranular texture (Fig. 2). It is dominated by subhedral clinopyroxene and olivine, and frequently lath-shaped plagioclase (now diaplectic glass; maskelynite). Minor to accessory phases include ilmenite, Ti-poor magnetite, orthopyroxene, chromite, pyrrhotite, silica, and Cl-apatite. Limited terrestrial weathering is apparent, with heterogeneously distributed calcite veining and rare phyllosilicate alteration of pyrrhotite and olivine.

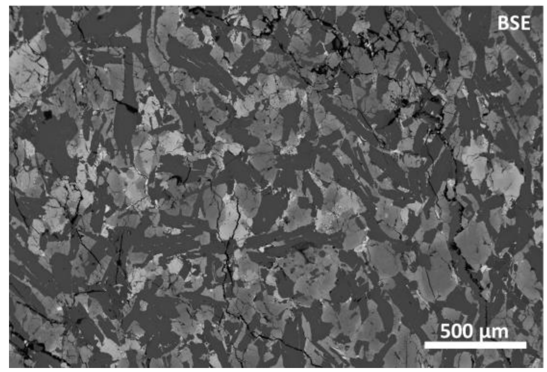

Fig. 2: *Typical variably intergranular texture of NWA 13467. Dark grey, maskelynite; mid-grey, augite; light grey, olivine.*

Clinopyroxene: Zoned, subhedral grains of augite are dominant in NWA 13467. No pigeonite was observed, though rarely subcalcic augite is present (Fig. 3). Some augite cores (Mg# ~53) retain faint oscillatory and/or complex zonation. Calcium- and Fe-rich rims are texturally distinct, and often possess abrupt rather than diffusive boundaries. No hedenbergite-fayalite-silica symplectites expected from the breakdown of meta-stable pyroxferroite were observed.

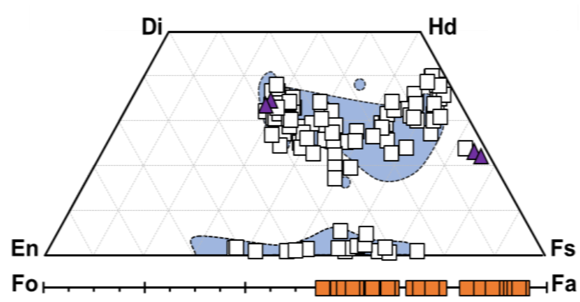

Fig. 3: *NWA 13467 pyroxene (white squares; n=103) and olivine (orange squares; n=45) compositions. NWA 8159 (blue fields [3]) and NWA 7635 (purple triangles[3,4]) pyroxene compositions are also shown.*

Olivine: NWA 13467 olivine is fayalitic (Fig. 3), and typically shows core-to-rim zonation (Fig. 4) with decreasing Mg#, CaO and Cr_2O_3 with increasing MnO. Widespread breakdown to orthopyroxene-magnetite symplectites (Fig. 4) is apparent in all olivine grains.

Orthopyroxene-magnetite symplectites are dominantly focused at the boundaries of olivine, but often ingress into olivine grains, ostensibly along fracture-aided reaction fronts. Augite in direct contact with olivine zone to orthopyroxene or Ca-rich rims, and are distinct from breakdown textures (Fig. 4).

Plagioclase: Plagioclase in NWA 13467 yields a range in compositions of $An_{41.9\text{-}61.4}Ab_{38.1\text{-}57.3}Or_{0.1\text{-}1.2}$. Complete transformation of plagioclase to maskelynite has been previously reported [8].

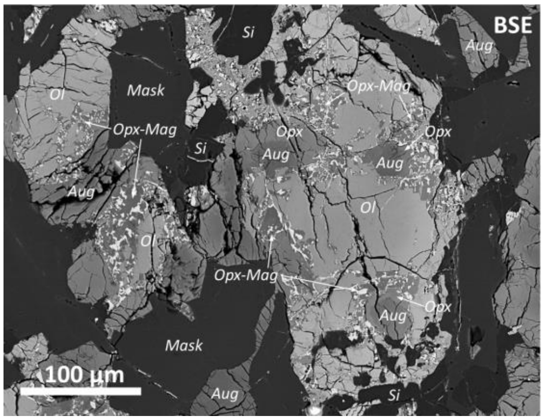

Fig. 4: *NWA 13467 olivine with breakdown to orthopyroxene-magnetite symplectites. Ol; olivine, Aug; augite, Opx; orthopyroxene, Mask; maskelynite, Mag; magnetite, and Si; silica.*

Oxides: NWA 13467 has a diverse oxide assemblage. Zinc-bearing (average 0.7 wt.% ZnO) chromite (≤50 µm; Cr# ~68) are observed within and associated with olivine. Chromite are poor in ferric iron (average $100xFe^{3+}$/totalFe; 6.7). Both ilmenite and magnetite are present as discrete phases and within mesostasis; magnetite possess near end-member compositions, typically yielding <1 wt.% TiO_2, and are commonly observed overprinting pyrrhotite. Despite the presence of near end-member magnetite, ilmenite yield low hematite end-member contents of <10.

Late-stage phases: Pockets of mesostasis are abundant, and contain lobate skeletal ilmenite and Cl-apatite, with fayalite, magnetite and silica. Silica is present throughout, and may host blebs of pyrite or be strongly associated with olivine (Fig. 3). In contrast to most shergottites, no merrillite has been observed.

Shock metamorphism: NWA 13467 has experienced significant shock metamorphism. Shock features include: pervasive fracturing, assumed complete transformation of plagioclase to maskelynite, thin shock melt veins, and a large number of shock melt pockets. Shock melt pockets are often vesicular, with localized granular textures indicating nascent crystallization of silicates and sulphides from shock melt.

Discussion and Further Work: The fine-grained nature of NWA 13467, retention of subtle zonation in augite cores, and preservation of pyroxferroite compositions indicates rapid cooling upon emplacement at or near the martian surface. While chromite and ilmenite are poor in ferric iron, late-stage oxidation of NWA 13467 is shown by the presence of orthopyroxene-magnetite symplectites, formed by either peritectic or sub-solidus oxidation of olivine grains [3,9], and the replacement of pyrrhotite by near end-member magnetite. It is currently unclear whether oxidation represents magmatic or sub-solidus processes, but the limited reaction of chromite grains in direct contact with magnetite may indicate the latter.

An absence of pigeonite indicates NWA 13467 is distinct from late Amazonian shergottites [1], but highlights a potential affinity to ~2400 Ma augite-rich shergottites NWA 8159 and NWA 7635 [3,4]. While NWA 13467 is clearly texturally distinct from NWA 7635 [4], the variably intergranular texture of our sample shows significant similarity to coarser domains of NWA 8159 [3]. Orthopyroxene-magnetite symplectites were also unique to NWA 8159 [3,9]; further geochemical similarities include broadly comparable pyroxene compositions (Fig. 3) and near end-member magnetite [3,9]. However, differences are also apparent. These include the presence of sulphides in NWA 13467, and an absence of magnetite phenocrysts and olivine alteration [3]; the latter may reflect the lower weathering grade of NWA 13467. Our sample has also experienced significantly higher shock *P-T-t* conditions than NWA 8159, which is thought to have undergone bulk shock pressures of 15 to 23 GPa [3,10], and potentially NWA 7635 [4]. Ongoing geochemical investigation will therefore not only elucidate the source characteristics, crystallization age and cosmic ray exposure age of NWA 13467, but also test a genetic link to augite-rich shergottites or whether NWA 13467 represents a hithero unsampled portion of martian crust.

Acknowledgements: We are hugely grateful to Stuart Kearns for EPMA assistance and Geoff Long for sample preparation.

References: [1] Udry, A. et al. (2020). *JGR: Planets, 125*, e2020JE00652. [2] Agee, C.B. et al. (2013) *Science, 339,* 780-785. [3] Herd, C.D.K. et al. (2017) *GCA, 218,* 1-26. [4] Lapen, T.J. et al. (2017) *Sci. Adv., 3,* e1600922. [5] Filiberto, J. (2014) *Am. Min., 99,* 601-606. [6] Hewins, R.H. (2019). *MAPS, 54,* 2132-2148. [7] Costa, M.M. (2020). *PNAS, 117,* 3-973-30979. [8] NWA 13467, Meteoritical Bulletin 109. *The Meteoritical Society.* [9] Shearer, C.K. et al. (2019) *GCA, 258,* 242-257. [10] Sharp, T.G. et al. (2019) *GCA,* 246, *197-212.*